DC, AC and Noise Simulation of Organic Semiconductor Devices based on the Master Equation

Christoph Jungemann and Christoph Zimmermann
Chair of Electromagnetic Theory
RWTH Aachen University
52056 Aachen, Germany
Email: Jungemann@ieee.org

***Abstract*—The hopping transport in organic semiconductors produces characteristic frequency dependencies of the admittance and noise, which are calculated in this paper for the first time based on the master equation approach, where noise is evaluated by the Langevin approach and a modified Ramo-Shockley theorem. At low frequencies and low injection the non-equilibrium noise is found to be shot noise in the framework of this model.**

I. Introduction

In recent years organic light emitting diodes (OLEDs) have appeared in many applications and disordered organic semiconductors are the basis of various devices (e.g. [1]). Charge carrier transport in amorphous organic semiconductors is due to hopping of electrons or holes from one molecular site to another and can be described by a Pauli master equation [2]. The hopping rate depends on the total energy of the site, which includes the site energy and potential energy due to the quasi-static potential and image potential. The master equation is solved self-consistently with the Poisson equation for the quasi-static potential by the Newton-Raphson approach [3]. Here, we present for the first time small-signal and noise analyses, which are performed directly in the frequency domain. This enables simulation of admittance spectroscopy, a powerful tool to investigate transport in organic semiconductor devices.

II. Model

The transport model is the same as in Refs. [2], [3]. A 3D tensor-product grid with a constant and isotropic spacing of a_0 is assumed for the hopping sites, where the x direction is the transport direction. The device is a simple unipolar 1D diode with contacts at the left and right-hand sides of a homogeneous semiconductor bulk with the permittivity ε. The length of the diode is L and its cross section A. The master equation for the 3D grid is

$$\frac{dp_i}{dt} + \sum_j \left[(1-p_j)\, v_{ji} p_i - (1-p_i)\, v_{ij} p_j \right] = 0 \; . \quad (1)$$

p_i is the occupancy of site i, of which the energies are randomly distributed according to a Gaussian distribution, and v_{ij} is the transition rate for hopping from site j to i, which is given by the Miller-Abrahams expression [2]. Scattering is possible within a sphere with a radius of $\sqrt{3}a_0$. The model and device parameters are the same as for Fig. 1(a) of Ref. [2] and the boundary conditions of the master equation are taken from Ref. [3], where the occupancy is fixed to 0.5 on the contacts and periodic boundary conditions are used on the other surfaces. The master equation is solved together with a 1D Poisson equation, in which the particle density is averaged over the cross section perpendicular to the transport direction and the potential is constant within a cross section.

In Ref. [4] it is shown that the Pauli master equation violates current continuity, because the particles hop instantaneously from one site to the next. This corresponds to the annihilation of a particle at site i and immediate creation at site j, and the total current density $\vec{J} + \partial\vec{D}/\partial t$ is no longer divergenceless

$$\mathrm{div}\left(\vec{J} + \frac{\partial \vec{D}}{\partial t}\right) = q\,(1-p_j)\, v_{ji} p_i \left[\delta\left(\vec{r}-\vec{r}_j\right) - \delta\left(\vec{r}-\vec{r}_i\right)\right] \quad (2)$$

and the conduction current density $\vec{J}$ is zero. $\vec{r}_i$ is the location of the site i and q the particle charge. In order to evaluate the terminal current with the Ramo-Shockley theorem [5], which is based on a divergencelass total current density, it has to be modified for hopping, which results in generation/recombination [6]. The current flowing into terminal l is given by the integral over the terminal area ∂D_l

$$I_l = -\int_{\partial D_l} \left(\vec{J} + \frac{\partial \vec{D}}{\partial t}\right) \cdot d\vec{A} \; , \quad (3)$$

where $d\vec{A}$ has an outwards orientation. With the fundamental solution $h_l(\vec{r})$ for terminal l of the Poisson equation for zero space charge and a modified boundary condition for the terminals $h_l(\vec{r} \in \partial D_k) = \delta_{l,k}$ the integral can be extended to the complete surface of the device ∂D

$$I_l = -\oint_{\partial D} h_l \left(\vec{J} + \frac{\partial \vec{D}}{\partial t}\right) \cdot d\vec{A} \; , \quad (4)$$

where it is assumed that Neumann-type boundary conditions apply to all non-contact areas. With Gauss' law we obtain an integral over the volume of the device D [6]

$$I_l = -\int_D \mathrm{div}\left[h_l \left(\vec{J} + \frac{\partial \vec{D}}{\partial t}\right)\right] dV$$

978-1-4799-5288-5/14/$31.00 © 2014 IEEE

$$= -\int_D \mathrm{grad} h_l \cdot \left(\vec{J} + \frac{\partial \vec{D}}{\partial t} \right) + h_l \mathrm{div} \left(\vec{J} + \frac{\partial \vec{D}}{\partial t} \right) dV \quad (5)$$

In the last line the first term almost completely vanishes, because the conduction current density is zero and the special choice of the test function h_l cancels the displacement current due to the space charge and only the contribution due to the electrostatic capacitance C_{lk} remains [5]

$$I_l = \sum_k C_{lk} \frac{dV_k}{dt} - \int_D h_l \mathrm{div} \left(\vec{J} + \frac{\partial \vec{D}}{\partial t} \right) dV \ , \quad (6)$$

where the sum runs over all terminals and V_k is the bias applied to the terminal k. In the case of the diode the left terminal is grounded and the bias V is applied between the right and left terminals. The test function is given in this case by $h(\vec{r}) = x/L$ and the modified Ramo-Shockley theorem evaluates for the right-hand side terminal to

$$I = C \frac{dV}{dt} + \sum_{i,j} q \left(1 - p_j\right) v_{ji} p_i \frac{x_i - x_j}{L} \ . \quad (7)$$

x_i is the x-coordinate of site i and $C = \varepsilon A / L$.

Small-signal analysis is performed under the sinusoidal steady-state condition for an angular frequency ω with a master equation, which is linearized w.r.t. the stationary state (p_i is the DC occupancy)

$$\begin{aligned} \mathrm{j}\omega \underline{p}_i + \sum_j \Bigg[& \left(1 - p_j\right) v_{ji} \underline{p}_i - \underline{p}_j v_{ji} p_i \\ & + \left(1 - p_j\right) \left(\frac{\partial v_{ji}}{\partial \varphi_i} \underline{\varphi}_i + \frac{\partial v_{ji}}{\partial \varphi_j} \underline{\varphi}_j \right) p_i \\ & - \left(1 - p_i\right) v_{ij} \underline{p}_j + \underline{p}_i v_{ij} p_j \\ & - \left(1 - p_i\right) \left(\frac{\partial v_{ij}}{\partial \varphi_i} \underline{\varphi}_i + \frac{\partial v_{ij}}{\partial \varphi_j} \underline{\varphi}_j \right) p_j \Bigg] = 0 \ , \end{aligned} \quad (8)$$

where $\underline{p}_i$ is the phasor of the small-signal occupancy, and $\underline{\varphi}_i$ the phasor of the quasi-static potential, which is the solution of the small-signal Poisson equation. The admittance parameters are calculated with the linearized version of the modified Ramo-Shockley theorem (7).

Noise is calculated based on the Langevin approach for the master equation. The power spectral density (PSD) of the Langevin forces is given by twice the hopping frequency, because hopping is a Poisson process similar to scattering or generation/recombination [7], [8]. The transfer function $\underline{G}_k$ of the terminal current due to the generation of a particle at site k, is calculated by solving the linearized system for a Kronecker function $\delta_{i,k}$ on the right-hand side of (8) together with the small-signal Poisson equation by the adjoint method [9]. The PSD of the terminal current is given with the linearization of the modified Ramo-Shockley theorem (7) by

$$S_{II} = \sum_i \sum_{j \neq i} 2q^2 \left| \underline{G}_i - \underline{G}_j - \frac{x_i - x_j}{L} \right|^2 \left(1 - p_j\right) v_{ji} p_i \ , \quad (9)$$

where the creation at site j and annihilation at site i is explicitly taken into account, because this is not captured by the transfer functions $\underline{G}_i$, $\underline{G}_j$.

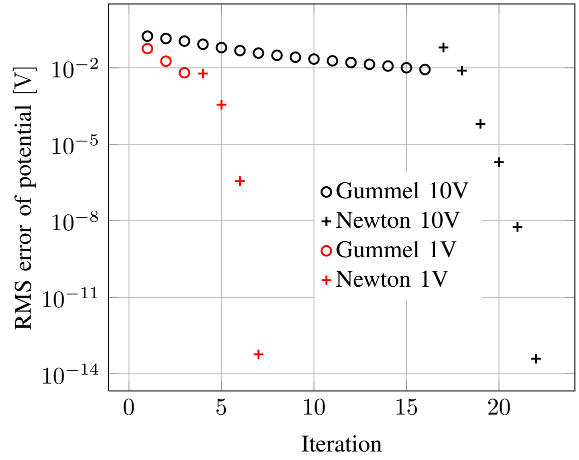

Fig. 1. Convergence of the algorithm for the device of Fig. 1(a) in Ref. [2] at a temperature of 295K.

To obtain a stationary solution, first the Poisson equation is solved, where the particle density is calculated based on the Fermi-Dirac distribution and a Fermi energy, which linearly varies between the two contacts. At equilibrium this yields already the correct solution. In a second step a Gummel iteration of the Poisson and master equations is performed, where the Poisson equation is solved under the assumption of a constant quasi-Fermi level for the charge carriers [10]. The iteration is stopped, when the RMS error of the potential is less than 10mV. In the last step, a full Newton-Raphson approach is used to solve both equations simultaneously [3]. The algorithm stops, when the RMS error of the potential is smaller than 10^{-10}V. In Fig. 1 two examples are shown for different voltages. The algorithm converges well and the Newton-Raphson method shows quadratic convergence. In the case of low temperatures (e.g. 77K) it might be necessary to run the Gummel iteration to a lower limit, before the Newton-Raphson approach can converge.

III. Simulation Results

The absolute value of the current and bias is used in all figures for the sake of convenience and the results do not depend on whether holes or electrons are simulated. The device with the parameters given for Fig. 1(a) in Ref. [2] is investigated. The terminal current of this device is shown in Fig. 2 for four injection barriers and the results agree very well with the ones in Ref. [2]. The CPU time for a single step of the Newton-Raphson method is less than two minutes on a single core of a current CPU for $65 \times 100 \times 100$ sites, where the linear system is solved with ILUPACK [11]. The particle density (Fig. 3) varies strongly due to the different injection barriers. The randomly chosen site energies are in all simulations the same and they induce similar fluctuations in all four cases. In the vicinity of the contacts the particle density is increased by the image potential. In the case of the two lowest barriers the particle density within the device is large enough to have an impact on the potential (Fig. 4).

The small-signal conductance $G(f) = \Re\{\underline{Y}(2\pi f)\}$ (Fig.5) and capacitance $C(f) = \Im\{\underline{Y}(2\pi f)/2\pi f\}$ (Fig.6) for an injection barrier of 0eV show a strong dependence on frequency revealing new information about the transport within

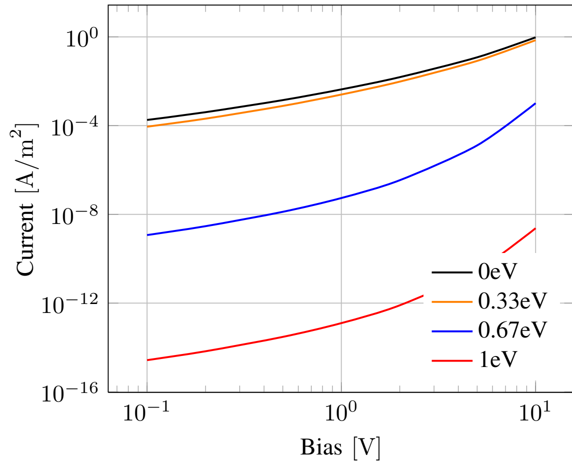

Fig. 2. Terminal currents for the device of Fig. 1(a) in Ref. [2] for different injection barriers at 295K.

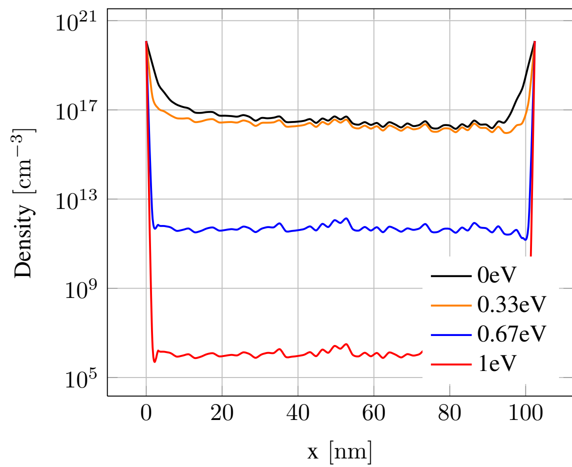

Fig. 3. Hole density for the device of Fig. 1(a) in Ref. [2] for different injection barriers at 295K and a bias of 1V.

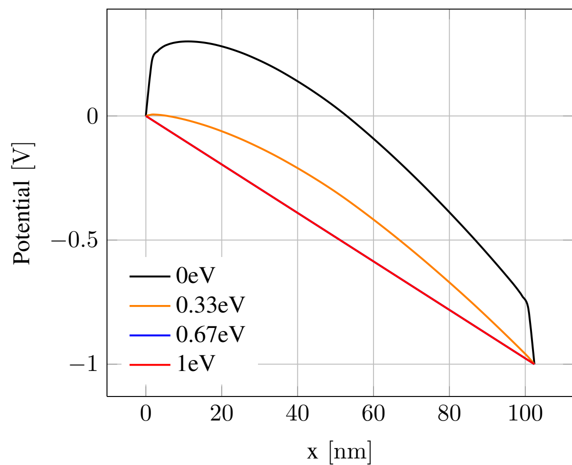

Fig. 4. Potential for the device of Fig. 1(a) in Ref. [2] for different injection barriers at 295K and a bias of 1V.

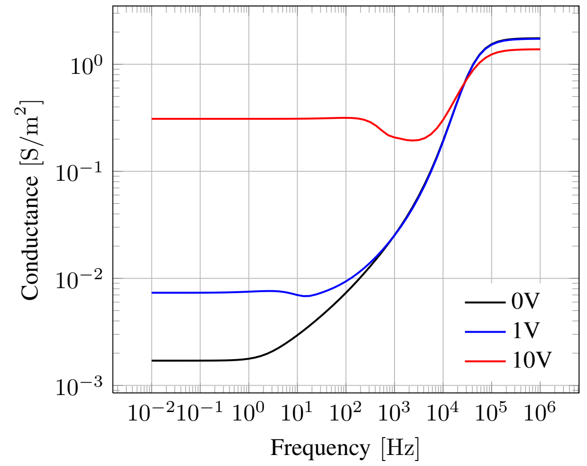

Fig. 5. Conductance for an injection barrier of 0eV at 295K.

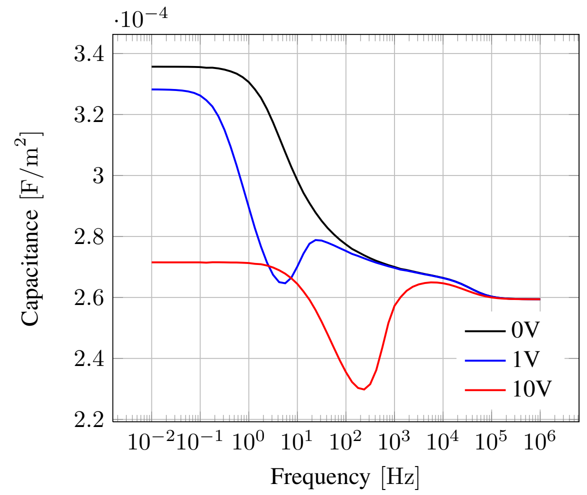

Fig. 6. Capacitance for an injection barrier of 0eV at 295K.

the device (e.g. transit time). Compared to transient large-signal simulations (e.g. Ref. [3]) the small-signal simulations are more easily interpreted and contain more information, since they also depend on the DC bias.

Another source for information on the transport processes within a device is terminal current noise (Fig. 7). It shows a strong dependence on frequency especially at low frequencies due to the rather slow transport processes. Under non-equilibrium conditions the noise contains additional information compared to the admittance as can be gathered from the noise temperature $T_\mathrm{n} = S_{jj}/4k_\mathrm{B}\Re\{Y\}$ (Fig. 8). Only in the case of equilibrium the noise is given by the Nyquist theorem ($T_\mathrm{n} = T_0$ = 295K) and no new information is obtained. For equilibrium the Nyquist theorem is satisfied by the numerical results with excellent accuracy validating our implementation. At sufficiently low frequencies we expect shot noise, because the particles cross a barrier when moving from the left to the right-hand side. In the case of the two larger contact barriers the barrier is located between the semiconductor and contact, whereas in the other two cases it is within the device due to the quasi-static potential (Fig. 4). In the latter case a certain suppression of the shot noise might occur due to

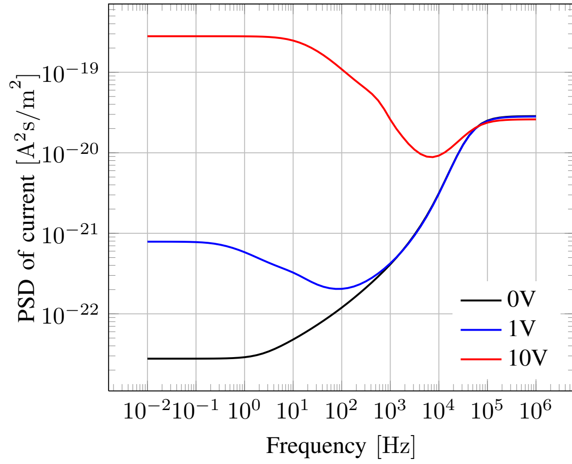

Fig. 7. Power spectral density of the terminal current for an injection barrier of 0eV at 295K.

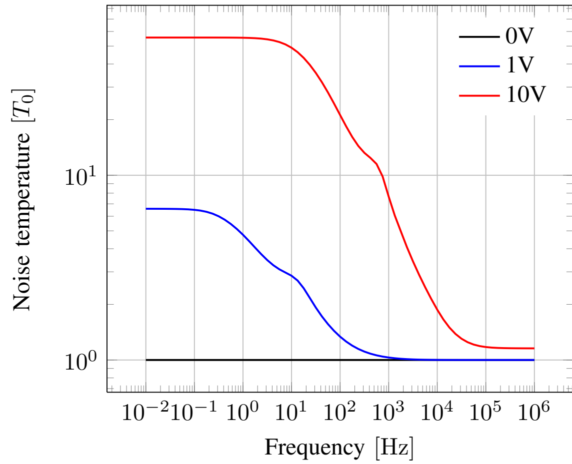

Fig. 8. Noise temperature for an injection barrier of 0eV at 295K.

Coulomb interaction between the particles. In Fig. 9 the PSD of the terminal current noise is shown at zero frequency. The noise rapidly approaches shot noise ($2qI$) for increasing bias (at zero bias thermal noise is obtained). Only in the case of very large currents (high injection) the noise is slightly modified by the interaction with the non-negligible space charge (Fig. 3). This expected behavior of the noise again validates our implementation.

IV. Conclusion

We have presented the first small-signal and noise calculations for organic semiconductor devices based on the master equation. The method shows good convergence and at equilibrium the Nyquist theorem is satisfied with excellent accuracy.

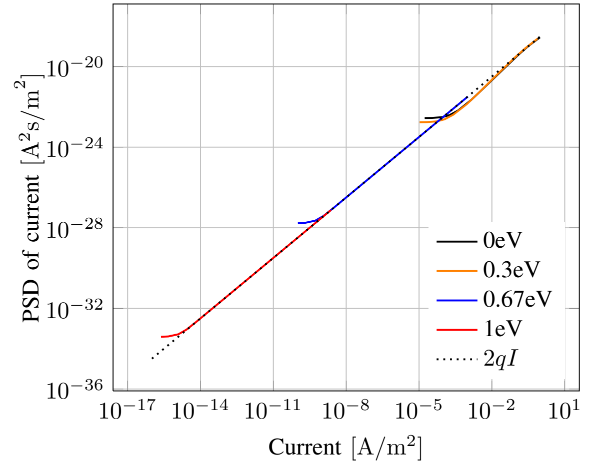

Fig. 9. Zero-frequency power spectral density of the terminal current for different injection barriers at 295K as a function of the current and shot noise.

References

[1] J. H. Burroughes, D. D. C. Bradley, A. R. Brown, R. N. Marks, K. Mackay, R. H. Friend, P. L. Burns, and A. B. Holmes, "Light-emitting diodes based on conjugated polymers," *Nature*, vol. 347, pp. 539 – 541, 1990.

[2] J. J. M. van der Holst, M. A. Uijttewaal, B. Ramachandhran, R. Coehoorn, P. A. Bobbert, G. A. de Wijs, and R. A. de Groot, "Modeling and analysis of the three-dimensional current density in sandwich-type single-carrier devices of disordered organic semiconductors," *Phys. Rev. B*, vol. 79, p. 085203, Feb 2009. [Online]. Available: http://link.aps.org/doi/10.1103/PhysRevB.79.085203

[3] M. Szymanski, B. Luszczynska, and D. Djurado, "Modeling the transient space-charge-limited current response of organic semiconductor diodes using the master equation approach," *Selected Topics in Quantum Electronics, IEEE Journal of*, vol. 19, no. 5, pp. 1–7, Sept 2013.

[4] W. R. Frensley, "Boundary conditions for open quantum systems driven far from equilibrium," *Rev. Mod. Phys.*, vol. 62, pp. 745–791, Jul 1990. [Online]. Available: http://link.aps.org/doi/10.1103/RevModPhys.62.745

[5] H. Kim, H. S. Min, T. W. Tang, and Y. J. Park, "An extended proof of the Ramo-Shockley theorem," *Solid–State Electron.*, vol. 34, pp. 1251–1253, 1991.

[6] P. D. Yoder, K. Gärtner, and W. Fichtner, "A generalized Ramo-Shockley theorem for classical to quantum transport at arbitrary frequencies," *J. Appl. Phys.*, vol. 79, pp. 1951–1954, 1996.

[7] S. Kogan, *Electronic Noise and Fluctuations in Solids*. Cambridge, New York, Melbourne: Cambridge University Press, 1996.

[8] F. Bonani and G. Ghione, *Noise in Semiconductor Devices, Modeling and Simulation*, ser. Advanced Microelectronics. Berlin, Heidelberg, New York: Springer, 2001.

[9] F. H. Branin, "Network sensitivity and noise analysis simplified," *IEEE Transactions on circuit theory*, vol. 20, pp. 285–288, 1973.

[10] H. K. Gummel, "A self-consistent iterative scheme for one-dimensional steady state transistor calculations," *Electron Devices, IEEE Transactions on*, pp. 455–465, October 1964.

[11] M. Bollhöfer and Y. Saad, "Multilevel preconditioners constructed from inverse–based ILUs," *SIAM J. Sci. Comput.*, vol. 27, no. 5, pp. 1627–1650, 2006.